

# Addition of $\alpha$ A-Crystallin Sequence 164–173 to a Mini-Chaperone DFVIFLDVKHFSPEDLT Alters the Conformation but Not the Chaperone-like Activity

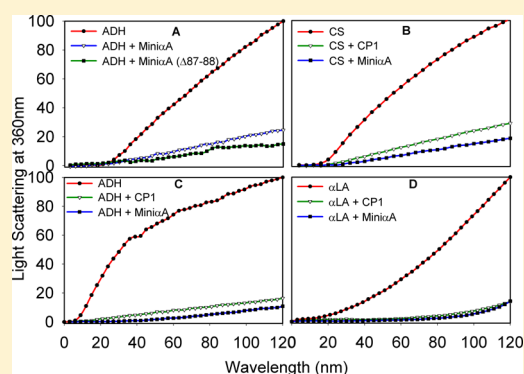
Murugesan Raju,<sup>†</sup> Puttur Santhoshkumar,<sup>†</sup> Leike Xie,<sup>†</sup> and K. Krishna Sharma<sup>\*,†,‡</sup>

<sup>†</sup>Department of Ophthalmology, University of Missouri–Columbia School of Medicine, Columbia, Missouri 65212, United States

<sup>‡</sup>Department of Biochemistry, University of Missouri–Columbia School of Medicine, Columbia, Missouri 65212, United States

## Supporting Information

**ABSTRACT:** It has been shown that  $\alpha$ A-mini-chaperone, a peptide representing the chaperone binding site in  $\alpha$ A-crystallin, prevents destabilized protein aggregation.  $\alpha$ A-Mini-chaperone has been shown to form amyloid fibrils. This study was undertaken to improve the stability of  $\alpha$ A-mini-chaperone while preserving its anti-aggregation activity by fusing the flexible and solvent-exposed C-terminal 164–173 region of  $\alpha$ A-crystallin to the mini-chaperone sequence DFVIFLDVKHFSPEDLT. The resulting chimeric chaperone peptide, DFVIFLDVKHFSPEDLTEEKPTS-APSS (designated CP1), was characterized. Circular dichroism studies showed that unlike  $\alpha$ A-mini-chaperone with its  $\beta$ -sheet structure, the CP1 peptide exhibited a random structure. Transmission electron microscopy (TEM) examination of the CP1 peptide incubated in a shaker at 37 °C for 72 h did not reveal amyloid fibrils, whereas  $\alpha$ A-mini-chaperone showed distinct fibrils. Consistent with TEM observation, the thioflavin T binding assay showed an increased level of dye binding in the mini-chaperone incubated at 37 °C and subjected to shaking but not of the CP1 peptide incubated under similar conditions. The chaperone activity of the CP1 peptide was comparable to that of  $\alpha$ A-mini-chaperone against denaturing alcohol dehydrogenase, citrate synthase, and  $\alpha$ -lactalbumin. Transduction of both peptide chaperones to COS-7 cells showed no cytotoxic effects. The antioxidation assay involving the H<sub>2</sub>O<sub>2</sub> treatment of COS-7 cells revealed that  $\alpha$ A-mini-chaperone and the CP1 peptide have comparable cytoprotective properties against H<sub>2</sub>O<sub>2</sub>-induced oxidative damage in COS-7 cells. This study therefore shows that the addition of C-terminal sequence 164–173 of  $\alpha$ A-crystallin to  $\alpha$ A-mini-chaperone influences the conformation of  $\alpha$ A-mini-chaperone without affecting its chaperone function or cytoprotective activity.



Peptides such as vasopressin analogues, oxytocin analogue, angiotensin II receptor antagonist, antimicrobial peptides, and antidiabetic peptides are widely used as therapeutic molecules in the management of pathological conditions.<sup>1,2</sup> Our laboratory identified a 19-amino acid sequence (<sup>70</sup>KFVIFLDVKHFSPEDLTVK<sup>88</sup>) in chaperone protein  $\alpha$ A-crystallin that can suppress aggregation of denaturing proteins, and we called this peptide “ $\alpha$ A-mini-chaperone”.<sup>3</sup> The mini-chaperone was shown to prevent aggregation of proteins denatured by heat, oxidation, and chemical methods. In addition,  $\alpha$ A-mini-chaperone was shown to prevent aggregation of heat-induced denatured alcohol dehydrogenase (ADH),<sup>3</sup> oxidation and ultraviolet (UV)-induced aggregation of  $\gamma$ -crystallins,<sup>4</sup> and dithiothreitol (DTT)-induced unfolding and aggregation of  $\alpha$ -lactalbumin and insulin.<sup>5</sup> Further, the mini-chaperone was shown to have the ability to inhibit  $\beta$ -amyloid fibril formation and toxicity to pheochromocytoma (PC12) cells.<sup>6</sup> Recent work in our laboratory also showed that  $\alpha$ A-mini-chaperone can stabilize the mutant  $\alpha$ AG98R-crystallin and rescue its chaperone activity<sup>7</sup> and can bind metal ion.<sup>8</sup> Others have shown that  $\alpha$ A-crymini-chaperone protects retinal pigment

epithelium (RPE) cells from oxidative damage.<sup>9,10</sup> Using RPE cells, it was demonstrated that  $\alpha$ B-crystallin has both cytosolic and nuclear anti-apoptotic roles.<sup>11</sup> While apoptosis in cardiac H9c2 cells was prevented by  $\alpha$ B-crystallin,<sup>12</sup>  $\alpha$ A-crystallin was effective against Bax-induced apoptosis in cone-derived 661W cells.<sup>13</sup> Studies have shown that acetylation of  $\alpha$ B-crystallin enhances both chaperone and anti-apoptotic activities,<sup>14</sup> and the extent of heat and oxidative stress-induced death in lens cells will be diminished after treatment with cell-penetrating  $\alpha$ -crystallin.<sup>15</sup> It has been shown that  $\alpha$ A-mini-chaperone inhibits selenite-induced cataract in rats.<sup>16</sup> Together, these studies suggest that  $\alpha$ A- and  $\alpha$ B-crystallin and  $\alpha$ A-mini-chaperone have the potential to become therapeutic molecules for diseases associated with protein aggregation. The amino acid sequence corresponding to the mini-chaperone is highly conserved across the crystallin domain of small heat shock proteins (sHSPs) and

Received: December 31, 2013

Revised: April 2, 2014

Published: April 3, 2014

Table I. Peptide Chaperones Used in This Study

peptide	sequence
$\alpha$ A-mini-chaperone	DFVIFLDVKHFSPEDLTVK
chimeric peptide chaperone (CP1)	DFVIFLDVKHFSPEDLTEEKPTSAPSS
CP1- $\Delta$ 172–173 peptide-1	DFVIFLDVKHFSPEDLTEEKPTSAP
CP1- $\Delta$ 170–173 peptide-2	DFVIFLDVKHFSPEDLTEEKPTS
CP1- $\Delta$ 168–173 peptide-3	DFVIFLDVKHFSPEDLTEEKPT
CP1- $\Delta$ 166–173 peptide-4	DFVIFLDVKHFSPEDLTEE
$\alpha$ A-mini-chaperone $\Delta$ 87–88	DFVIFLDVKHFSPEDLT
$\alpha$ A-mini-chaperone-extended	DFVIFLDVKHFSPEDLTVKVKQEDFVEI

is rich in hydrophobic residues.<sup>17</sup> Secondary structural analysis of the  $\alpha$ -crystallin domain in sHSPs shows several regions with the propensity to form  $\beta$ -sheet structure(s). The mini-chaperone sequence aligns with the  $\beta$ 3 and  $\beta$ 4 region in human  $\alpha$ A-crystallin.  $\beta$ -Sheet rich, hydrophobic sequences are prone to forming amyloid fibrils.<sup>18,19</sup> It has been reported that  $\alpha$ A-crystallin subjected to partial denaturation forms amyloid fibrils *in vitro*.<sup>20</sup> Tanaka et al.<sup>21,23</sup> and others<sup>22</sup> have demonstrated that shaking the mini-chaperone  $\alpha$ A71–88 at 900 rpm for several hours leads to the formation of amyloid fibril-like aggregates that bind thioflavin T. Tanaka et al. have suggested that “the chaperone-like activity of  $\alpha$ AC-peptides could be correlated with their propensity to form amyloid fibrils”<sup>21</sup> and demonstrated increased chaperone activity in the fibril form of the  $\alpha$ A71–88 peptide.<sup>23</sup>

While our understanding of the structure and function of  $\alpha$ A- and  $\alpha$ B-crystallin remains incomplete, the C-terminal extensions of  $\alpha$ A- and  $\alpha$ B-crystallin have been characterized as largely unstructured and highly solvent-exposed.<sup>24,25</sup> The unstructured C-terminal region is believed to play a role in keeping the oligomer protein complexes as well as  $\alpha$ -crystallin–client protein complexes in their soluble forms. The removal of the C-terminal region of  $\alpha$ A-crystallin leads to decreased solubility,<sup>26,27</sup> and  $\alpha$ A-crystallin truncated at the C-terminus has reduced chaperone activity,<sup>28</sup> likely because of the reduced stability of the chaperone–client protein complex. We hypothesized that the addition of the C-terminal sequence of  $\alpha$ A-crystallin to  $\alpha$ A-mini-chaperone may enhance the solubility of the  $\alpha$ A-mini-chaperone–client protein complex. Further, we reasoned that because the C-terminal EEKPTSAPSS sequence of  $\alpha$ A-crystallin is hydrophilic, it might diminish the extent of fibril formation in the chimeric chaperone formed by the fusion of the  $\alpha$ A-mini-chaperone sequence and EEKPTSAPSS. Our earlier studies showed that the presence of a large part of the  $\alpha$ A-mini-chaperone is essential for its activity.<sup>3,4,8</sup> We therefore retained the core sequence of  $\alpha$ A-mini-chaperone in the chimeric chaperone peptide (CP1), created by the fusion of  $\alpha$ A-crystallin C-terminal residues EEKPTSAPSS to the C-terminal region of  $\alpha$ A-mini-chaperone sequence DFVIFLDV-KHFSPEDLT. Here, we show that CP1 displays anti-aggregation activity, as we expected, when tested with client proteins denatured by heat or chemical agents and does not form fibrils after agitation for an extended period of time. We also show that CP1 protects COS-7 cells from H<sub>2</sub>O<sub>2</sub>-induced apoptosis.

## MATERIALS AND METHODS

**Peptide and Proteins.** Peptides used in this study (Table I) were supplied by Genscript Corp. (Piscataway, NJ). These peptides were >95% pure according to HPLC and mass spectrometry. ADH, citrate synthase (CS), and  $\alpha$ -lactalbumin

(LA) were procured from Sigma-Aldrich (St. Louis, MO). Recombinant  $\alpha$ A-crystallin was expressed and purified as described previously.<sup>29</sup>

**Chaperone Assay.** To test whether the addition of the C-terminal sequence to  $\alpha$ A-mini-chaperone modulates its chaperone function,  $\alpha$ A-mini-chaperone, CP1 peptide, and its truncated forms were challenged with denaturing client proteins. The ADH aggregation assay was performed using 5  $\mu$ M protein in 1 mL of 50 mM phosphate buffer [150 mM NaCl and 100 mM EDTA (pH 7.2)] in the absence and presence of either  $\alpha$ A-mini-chaperone or CP1 peptide (40  $\mu$ M) at 37 °C. The citrate synthase aggregation assay was performed using 4  $\mu$ M protein in 1 mL of 40 mM HEPES-KOH buffer (pH 7.0) in the absence of peptide and in the presence of either  $\alpha$ A-mini-chaperone or CP1 peptide (40  $\mu$ M). For the LA aggregation assay, bovine LA (1.2 mg) was dissolved in 1 mL of 50 mM phosphate buffer [100 mM NaCl and 1 mM EDTA (pH 7.4)], and the aggregation was initiated by the addition of 20  $\mu$ M DTT (final concentration) at 37 °C in the absence and presence of  $\alpha$ A-mini-chaperone or CP1 peptide. The extent of aggregation was monitored at 360 nm in a Shimadzu spectrophotometer equipped with a temperature controller and a multiwell holder, as described previously.<sup>29</sup> Representative samples were also examined under a transmission electron microscope using a staining procedure described below.  $\alpha$ A-Mini-chaperone and CP1 peptide incubated under chaperone assay conditions were also subjected to Sephadex G-50 gel filtration chromatography to determine whether these peptides formed aggregates in assay buffers.

### Incubation and Thioflavin T (ThT) Fluorescence Assay.

The ThT fluorescence assay is commonly used as a fluorescence probe to quantify the fibril content of amyloid peptide. The ThT assay was performed according to the method described previously.<sup>6</sup>  $\alpha$ A-Mini chaperone or CP1 peptide was prepared in 50 mM phosphate buffer (pH 7.20) and incubated at 37 or 42 °C while being shaken at 250 rpm for 72 h. The ThT binding fibril content of the samples was measured at 0 and 72 h. For the ThT assay, peptide samples and ThT (final concentration of 10  $\mu$ M) were mixed and incubated at 37 °C for 10 min. The fluorescence intensity of the sample was measured by excitation at 450 nm, and emission was recorded over the wavelength range of 450–550 nm with a bandwidth of 5 nm and a scan speed of 10 nm/min using 10 mm path length cuvettes. An emission maximum at 480 nm was recorded.

**Transmission Electron Microscopy Study.** The morphology of amyloid-like fibrils formed by the peptide chaperones was studied by transmission electron microscopy (TEM), following the procedure described previously.<sup>30</sup> Briefly, the peptides (1 mg/mL) were dissolved in phosphate buffer and incubated in a 37 °C shaker kept at 250 rpm. After 24 h, 5

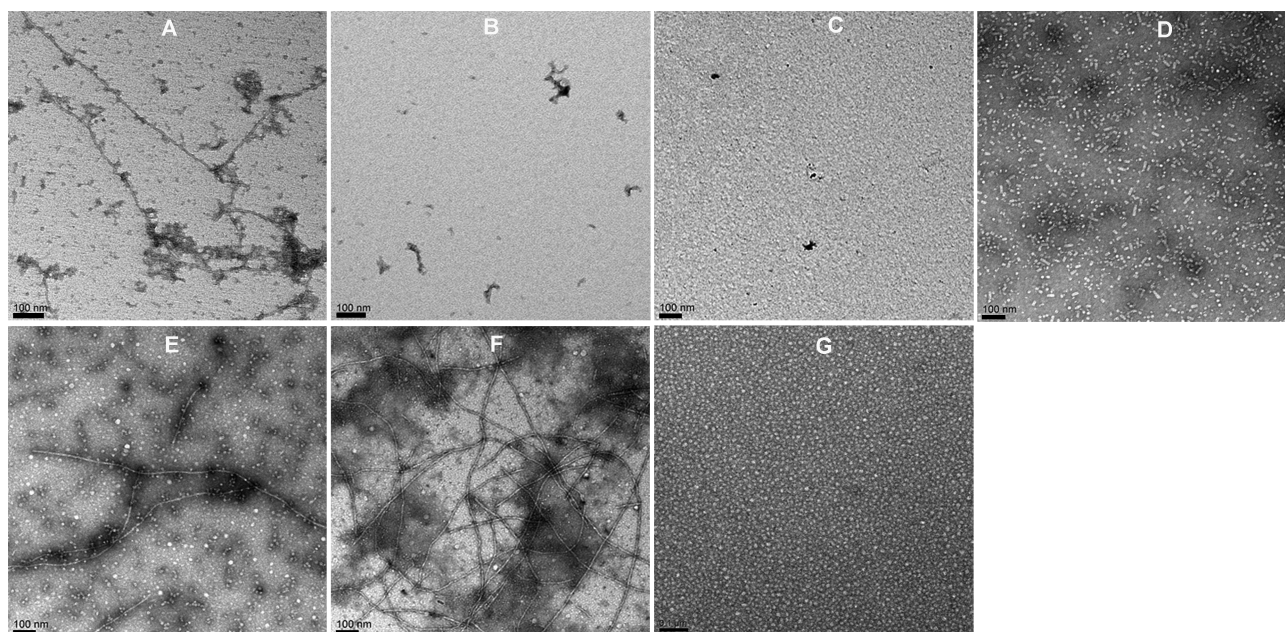


**Figure 1.** TEM images of chaperone peptides incubated at 37 °C. The peptide samples were incubated with a shaking incubator as described in Materials and Methods for 24 h: (A) mini- $\alpha$ A, (B) CP1, (C) CP1- $\Delta$ 172–173, (D) CP1- $\Delta$ 170–173, (E) CP1- $\Delta$ 168–173, (F) CP1- $\Delta$ 166–173, and (G)  $\alpha$ A70–96. The scale bar is 100 nm.

$\mu$ L aliquots were applied to carbon-coated 200 mesh copper grids at room temperature, stained with freshly prepared 2% uranyl acetate, and examined under a JEOL 1400 transmission electron microscope (120 kV). The images were obtained using digital imaging software from Gatam Digital Micrograph (Gatam, Inc., Warrendale, PA).

**Circular Dichroism (CD) Spectroscopy.** Far-ultraviolet (UV) CD spectra of  $\alpha$ A-mini-chaperone, CP1, and truncated CP1 were recorded using a Jasco (Easton, MD) J-815 CD spectropolarimeter. Peptides were prepared in 50 mM phosphate buffer (pH 7.2). Far-UV CD measurements were conducted over the wavelength range of 190–250 nm with a bandwidth of 0.5 nm and a scan speed of 10 nm/min using 2 mm path length cuvettes. All of the reported spectra were the cumulative averages of six scans after subtraction of the buffer blank.

**Bis-ANS Binding Studies.** The fluorescence of bis-ANS bound to peptides was measured using a Jasco FP750 spectrofluorometer. A bis-ANS solution (10  $\mu$ mol, equal to twice the amount required to saturate the binding sites) was added to a 0.1 mg/mL peptide solution in phosphate buffer (pH 7.2). The mixture was thoroughly mixed and then incubated for 10 min. Fluorescence emission spectra were then recorded at 400–600 nm using an excitation wavelength of 390 nm. The excitation and emission slits were set at 5 nm.

**Cell Culture Studies.** COS-7 cells and ARPE-19 cells were cultured in Dulbecco's modified Eagle's medium (DMEM), supplemented with 10% fetal bovine serum, 100 units/mL penicillin, and 100  $\mu$ g/mL streptomycin at 37 °C in an incubator with a 5% CO<sub>2</sub> atmosphere. Experiments were conducted in eight-well, sterile, clear-bottom slides. Cells were seeded at an appropriate density according to the experiments (25000 cells/cm<sup>2</sup>) and allowed to grow for 24 h, and then cells were exposed to 0–20  $\mu$ g/mL chaperone peptides in BioPorter (Sigma-Aldrich, St. Louis, MO) for 4 h in serum-free medium. In another set of experiments, 25–100  $\mu$ g/mL  $\alpha$ A-crystallin was used as a positive control chaperone. The chaperone

molecule-transduced cells were than exposed to H<sub>2</sub>O<sub>2</sub> (150  $\mu$ M) for 24 h. Appropriate control experiments were conducted simultaneously.

**TUNEL Assay.** The TdT-mediated digoxigenin-dUTP nick end labeling (TUNEL) assay for *in situ* apoptosis was performed according to the manufacturer's protocol (Chemicon, Temecula, CA). In brief, after H<sub>2</sub>O<sub>2</sub> (150  $\mu$ M) treatment in the absence and presence of chaperone molecules, cells were fixed in 4% paraformaldehyde overnight at 4 °C and washed twice with phosphate-buffered saline (PBS) for 5 min. Then the cells were postfixed in an ethanol/acetic acid mixture (2:1) for the permeability of TUNEL reagents into the cell nucleus. The 3' end labeling was conducted in a mixture containing terminal deoxynucleotidyl transferase, and incorporated 3' end labeling was detected using an anti-digoxigenin/rhodamine solution. The cells were observed under a fluorescence microscope (Leica DMR), and the images were recorded using an Optonics digital camera. The percentage of apoptotic cells was calculated by counting TUNEL-positive cells divided by total cells visualized in the given area.

**Flow Cytometry Analysis.** We used a fluorescein isothiocyanate (FITC)–annexin V apoptosis detection kit (BioLegend, San Diego, CA) for the cell apoptosis assay. Briefly, ARPE-19 cells (1  $\times$  10<sup>7</sup>) were treated with mini-chaperone peptides (20  $\mu$ g/mL) for 4 h in serum-free DMEM. After being treated, cells were washed with PBS twice and incubated for 24 h in serum-free medium in the presence of 150  $\mu$ M H<sub>2</sub>O<sub>2</sub>. The next day cells were trypsinized, washed twice with PO<sub>4</sub> buffer, and resuspended in 200  $\mu$ L of binding buffer containing 5  $\mu$ L of annexin V (10  $\mu$ g/mL) and 10  $\mu$ L of PI (20  $\mu$ g/mL). The mixtures were incubated for 15 min at room temperature. Stained cells were analyzed with a flow cytometer (BD FACScalibur) at the University of Missouri Cytology Core Facility. Cell Quest was used for data acquisition and analysis.

RESULTS

**Characterization of Mini-Chaperones.** Synthetic peptides  $\alpha$ A-mini-chaperone ( $\alpha$ A70–88),  $\alpha$ A-mini-chaperone  $\Delta$ 87–88 ( $\alpha$ A70–86),  $\alpha$ A-mini-chaperone-extended ( $\alpha$ A70–96), and CP1 peptide ( $\alpha$ A70–86+164–173) and the truncated forms of CP1 [peptide 1 (CP1- $\Delta$ 172–173), peptide 2 (CP1- $\Delta$ 170–173), peptide 3 (CP1- $\Delta$ 168–173), and peptide 4 (CP1- $\Delta$ 166–173)] were incubated (1 mg/mL) in PO<sub>4</sub> buffer at 37 °C in a shaker incubator set at 250 rpm. Samples were examined via TEM and the ThT binding assay after incubation for 24 and 72 h, respectively. The electron micrographs showed that  $\alpha$ A-mini-chaperone and truncated CP1 peptides, CP1- $\Delta$ 168–173 and CP1- $\Delta$ 166–173 assembled into unbranched fibrils  $\sim$ 7  $\pm$  1 nm in width and several millimeters in length (Figure 1A,E,F), whereas the CP1 peptide and the extended mini-chaperone peptide did not form fibrils or aggregates (Figure 1B,C,G). In contrast, CP1- $\Delta$ 170–173 displayed smaller proto-fibril-like aggregates (Figure 1D). As Figure 2

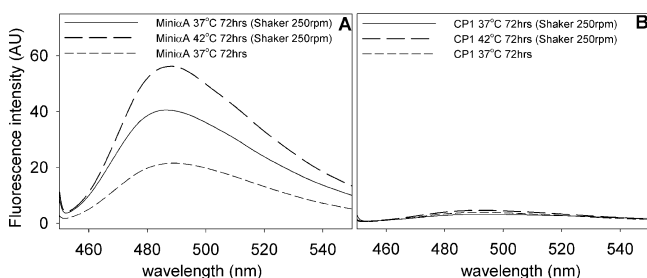
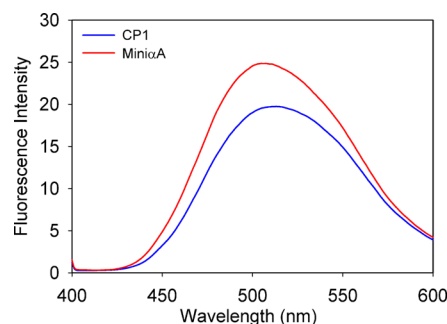


**Figure 2.** Thioflavin (ThT) fluorescence assay of peptide chaperones. Peptides were incubated at 37 or 42 °C for 72 h as described in Materials and Methods. ThT (final concentration of 10  $\mu$ M) was added following incubation with or without shaking, and the fluorescence spectra were recorded in a Jasco-750 spectrometer after excitation of the samples at 350 nm. (A) ThT fluorescence of mini- $\alpha$ A-chaperone, suggesting the presence of fibril-like structures. (B) Absence of ThT fluorescence with the CP1 peptide, indicating the absence of fibril-like structures.

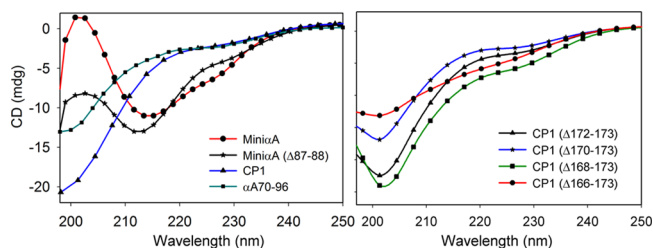
shows, no increase in ThT fluorescence occurred with CP1 peptide after incubation for 72 h, whereas  $\alpha$ A-mini-chaperone showed a 3-fold increase in ThT fluorescence under similar incubation conditions (Figure 2A).

Previous studies have shown that bis-ANS binding hydrophobic sites contribute to chaperone sites and that mini-chaperone binds bis-ANS. We therefore tested whether the addition of the  $\alpha$ A164–173 sequence (CP1) to mini- $\alpha$ A had any effect on bis-ANS binding. As shown in Figure 3, treatment of the CP1 peptide with bis-ANS and excitation at 390 nm generated a spectrum with emission maxima at 500 nm, similar to that of bis-ANS and the mini- $\alpha$ A peptide mixture but with a slightly lower fluorescence. However, the extended mini-chaperone showed a significant red shift in emission maxima in the bis-ANS spectrum, indicating minimal dye binding.

The far-UV CD spectrum of the  $\alpha$ A-mini-chaperone and its two-residue-truncated form exhibited maximal ellipticity at 216 and 214 nm, respectively, indicating that both peptides have a predominant  $\beta$ -sheet conformation at 25 °C (Figure 4). On the other hand, the far-UV CD profile of the CP1 peptide and its truncated forms as well as the mini-chaperone-extended peptide (Table I) showed maximal ellipticity at 200 nm, similar to the profile obtained when a peptide with a random conformation is analyzed by CD spectroscopy (Figure 4). A K2d program



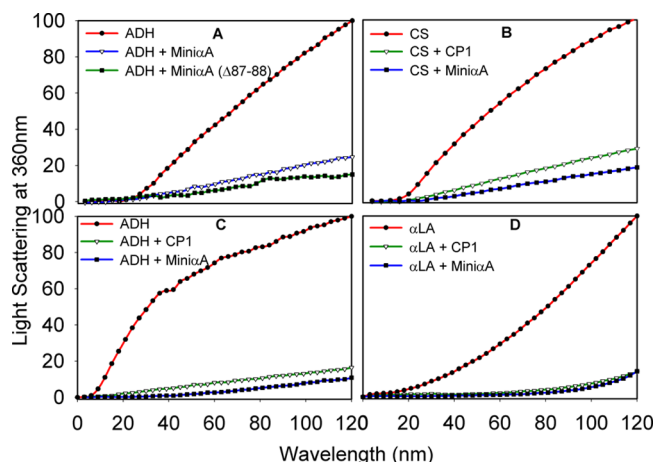
**Figure 3.** Fluorescence spectra of the hydrophobic fluorescent probe bis-ANS in the presence of peptide chaperones. The samples were excited at 390 nm, and emission was recorded at 520 nm.



**Figure 4.** Far-UV CD spectra of  $\alpha$ A-mini-chaperone and CP1 chaperone. The sequences of the peptide chaperones are given in Materials and Methods, as are the experimental conditions. Far-UV spectra of mini- $\alpha$ A (red), mini- $\alpha$ A ( $\Delta$ 87–88, black), and CP1 (blue). The right panel shows far-UV CD spectra of truncated CP1 peptides.

(Dichroweb) analysis performed on these peptide CD profiles confirmed that these peptides are largely in the random coil conformation (data not shown).

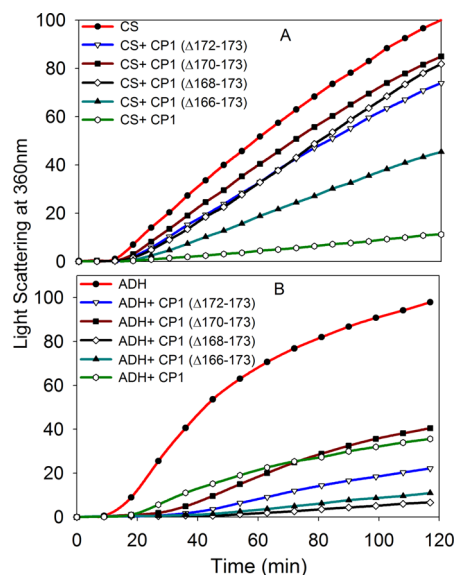
**Chaperone-like Activity of Mini-Chaperones.** We investigated the chaperone-like activity of the CP1 peptide to determine whether the addition of  $\alpha$ A-crystallin C-terminal residues had any effect on anti-aggregation activity. We also compared the chaperone activity of the CP1 peptide with that of  $\alpha$ A-mini-chaperone using three client proteins. Heat-induced aggregation of ADH and CS and DTT-induced lactalbumin aggregation were used to measure the chaperone-like activity of the peptides. When ADH was used as a client protein, the CP1 peptide showed dose-dependent suppression of aggregation of denaturing ADH (data not shown). Use of the CP1 peptide and ADH at a 1:8 ratio resulted in >90% suppression of light scattering. The kinetic curve shows comparable chaperone-like activity for the CP1 peptide and  $\alpha$ A-mini-chaperone (Figure 5). When the chaperone assay mixtures were examined via TEM after the assay, samples having CP1 or  $\alpha$ A-mini-chaperone and ADH showed similar profiles with negligible aggregates whereas a sample from denaturing ADH showed protein aggregates (data not shown). Heat-induced aggregation of CS was effectively (90%) prevented by 40  $\mu$ M CP1, and the extent of protection was similar to that of  $\alpha$ A-mini-chaperone and its truncated form. When we investigated the chaperone-like activity of the peptides against DTT-induced  $\alpha$ -lactalbumin aggregation, we found that 40  $\mu$ M  $\alpha$ A-mini-chaperone and CP1 peptide had comparable chaperone-like activity (Figure 5D). During all chaperone assays, the formation of light scattering particles by  $\alpha$ A-mini-chaperone, CP1, or  $\alpha$ A-mini-chaperone  $\Delta$ 87–88 was not observed. However, during Sephadex G 50 gel filtration studies,  $\alpha$ A-mini-chaperone eluted as two peaks, the first peak eluting immediately after the void volume and the



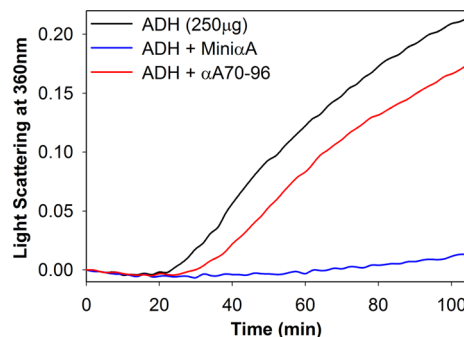
**Figure 5.** Aggregations of denaturing proteins in the presence of mini- $\alpha$ A-chaperone or chimeric mini-chaperone (CP1). (A) Heat- and EDTA-induced ADH ( $5 \mu\text{M}$ ) aggregation in the presence of mini- $\alpha$ A ( $40 \mu\text{M}$ ) or mini- $\alpha$ A ( $\Delta 87\text{--}88$ ,  $40 \mu\text{M}$ ) at  $37^\circ\text{C}$ . (B) Heat-induced citrate synthase ( $4 \mu\text{M}$ ) aggregation assay at  $43^\circ\text{C}$  in the presence of mini- $\alpha$ A ( $40 \mu\text{M}$ ) or CP1 ( $40 \mu\text{M}$ ). (C) ADH ( $5 \mu\text{M}$ ) aggregation in the presence of mini- $\alpha$ A ( $40 \mu\text{M}$ ) or CP1 ( $40 \mu\text{M}$ ). (D) Chaperone-like activity of mini- $\alpha$ A or CP1 peptide toward DDT-induced aggregation of LA at  $37^\circ\text{C}$ .

second peak corresponding to the monomeric form of the peptide elution region prior to incubation and as one peak, at the void volume region, after incubation for 2 h. This suggested that  $\alpha$ A-mini-chaperone is prone to aggregation (Figure 1 of the Supporting Information). Interestingly, the CP1 peptide chaperone did not show any evidence of aggregation before or after incubation at  $37^\circ\text{C}$  for 2 h because the peptide eluted from the Sephadex G-50 column at the expected elution time for the monomeric form of the peptide each time (Figure 1 of the Supporting Information). The chaperone activity of truncated forms of the CP1 peptide was also investigated with two substrates, ADH and CS (Figure 6). All four truncated forms of CP1 showed varying levels of chaperone activity. With ADH as a client protein, truncated CP1 peptides 1, 3, and 4 (Table 1) had increased activity compared to that of the CP1 peptide, whereas CP1 peptide 2 showed activity comparable to that of the CP1 peptide. However, when CS was used as a client protein, truncated CP1 peptides 1–4 displayed reduced anti-aggregation activity. Unlike the CP1 peptide, the extended  $\alpha$ A-mini-chaperone showed a  $>80\%$  loss of chaperone activity when tested with ADH as the client protein (Figure 7).

**Anti-Apoptotic Activity of Mini-Chaperones.** To study whether  $\alpha$ A-mini-chaperone and CP1 peptide offer protection against oxidative stress in mammalian cells, we incubated COS-7 cells with  $0\text{--}20 \mu\text{g/mL}$  chaperone peptides for 4 h in Bio-Porter, followed by  $150 \mu\text{M}$   $\text{H}_2\text{O}_2$ . In another set of experiments,  $25\text{--}100 \mu\text{g/mL}$   $\alpha$ A-crystallin was used in place of chaperone peptides. We selected this concentration for mini-chaperones because other studies have shown that  $\alpha$ A-mini-chaperone exerts protection against oxidative injury to RPE cells at this concentration.<sup>9</sup> Apoptotic cell death was assessed by the TUNEL assay. Our data show that both  $\alpha$ A-mini-chaperone and CP1 protected COS-7 cells from apoptotic cell death (Figure 8). This protection was highly significant ( $P < 0.01$ ) when compared to the cells treated with  $\text{H}_2\text{O}_2$  and without chaperone peptides. The dose-dependent effect of the peptide chaperone against  $\text{H}_2\text{O}_2$  treatment is also shown in



**Figure 6.** Effect of truncated CP1 peptides (CP1- $\Delta 172\text{--}173$ , CP1- $\Delta 170\text{--}173$ , CP1- $\Delta 168\text{--}173$ , and CP1- $\Delta 166\text{--}173$ ) on denaturing proteins. (A) Heat-induced CS ( $4 \mu\text{M}$ ) aggregation in the presence of truncated CP1 peptides ( $40 \mu\text{M}$ ) at  $43^\circ\text{C}$ . (B) Heat- and EDTA-induced ADH ( $5 \mu\text{M}$ ) aggregation assay at  $37^\circ\text{C}$  in the presence of truncated CP1 peptides ( $40 \mu\text{M}$ ).



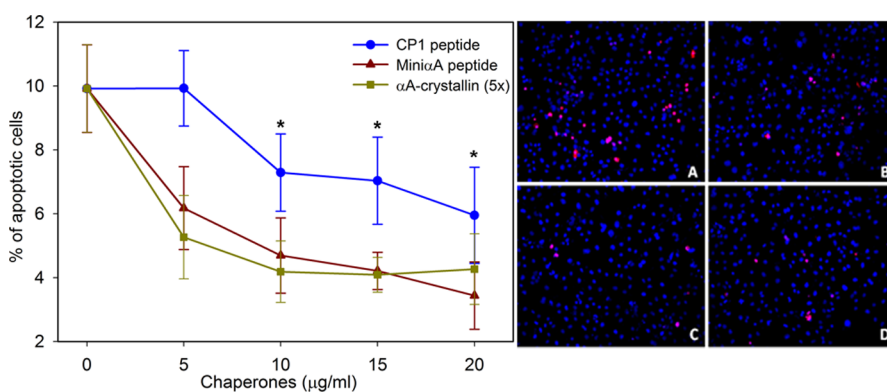
**Figure 7.** Heat- and EDTA-induced ADH ( $250 \mu\text{g}$ ) aggregation in the presence of mini- $\alpha$ A-chaperone ( $40 \mu\text{M}$ ) or mini- $\alpha$ A-extended peptide ( $40 \mu\text{M}$ ) at  $37^\circ\text{C}$ .

Figure 8. The CP1 peptide was less effective than the  $\alpha$ A-mini-chaperone, although it was protective.

To confirm the TUNEL results, in a separate experiment ARPE-19 cells were first treated with mini-chaperones, followed by oxidative agents. Apoptotic cells were probed using FITC-labeled Annexin V and nuclear stain propidium iodide (PI), for early and late apoptotic markers, respectively. The double-stained cells were analyzed by flow cytometry (Figure 9). The data show that mini-chaperones were effective in protecting against the  $\text{H}_2\text{O}_2$ -induced cell apoptotic cascade, consistent with the results from the TUNEL assay.

## DISCUSSION

**Effect of the Addition of the  $\alpha$ A-Crystallin C-Terminal Sequence to  $\alpha$ A-Mini-Chaperone.** Substitution of the C-terminal residues VK of  $\alpha$ A-mini-chaperone (DFVIFLDVVKH-FSPEDLTVK) with the  $\alpha$ A-crystallin C-terminal sequence EEKPTSAPSS decreased the pI of the peptide chaperone from 4.66 to 4.29. The pI was 4.15 when the  $\alpha$ A-mini-chaperone sequence was extended with the <sup>89</sup>VQEDFVEI<sup>96</sup> sequence of



**Figure 8.** Suppression of oxidant-induced cell death by  $\alpha$ A-mini-chaperone or CP1-chaperone. For the data displayed in the left panel, COS-7 cells were treated with 150  $\mu$ M H<sub>2</sub>O<sub>2</sub> and 0–20  $\mu$ g of either mini- $\alpha$ A or chimeric mini- $\alpha$ A for 3 h. Apoptosis was assessed by TUNEL staining, and the percentage of dead cells was quantified by counting grids. Asterisks indicate  $P < 0.01$  for mini- $\alpha$ A or CP1 at 10–20  $\mu$ g compared to control. The right panel shows TUNEL staining of the samples: (A) control, (B) CP1 (20  $\mu$ g/mL), (C)  $\alpha$ A-mini-chaperone (20  $\mu$ g/mL), and (D) wild-type  $\alpha$ A (100  $\mu$ g/mL).

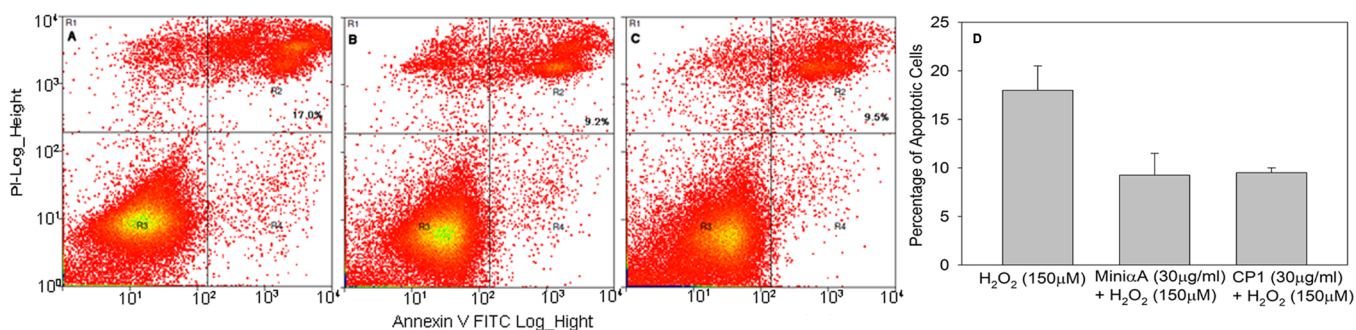


**Figure 9.** H<sub>2</sub>O<sub>2</sub>-induced cell apoptosis assay by flow cytometry, utilizing Annexin V vs propidium iodide (PI) staining. Cells in region R3 represent living cells (Annexin V-negative, PI-negative). Cells in region R2 represent late apoptotic cells (Annexin V-positive, PI-positive). Cells in region R1 represent early apoptotic cells (Annexin V-positive, PI-negative). Cells in region R4 represent damaged membranes only: (A) H<sub>2</sub>O<sub>2</sub> (150  $\mu$ M), (B) mini- $\alpha$ A (20  $\mu$ g/mL) with H<sub>2</sub>O<sub>2</sub>, and (C) CP1 (20  $\mu$ g/mL) with H<sub>2</sub>O<sub>2</sub>. (D) Average of three independent experiments.

$\alpha$ A-crystallin. We found no correlation between the pI value of the peptide and chaperone activity or secondary structure. When the extended mini-chaperone, CP1 peptide, and  $\alpha$ A-mini-chaperone were each incubated at 42 °C in a shaking incubator for 72 h under sterile conditions, the sample containing  $\alpha$ A-mini-chaperone developed cloudiness, whereas the CP1 peptide and the extended mini-chaperone solutions remained clear, suggesting that only  $\alpha$ A-mini-chaperone formed light scattering aggregates. The measurement of light scattering by the samples at 360 nm in a spectrophotometer confirmed the presence of light scattering in the  $\alpha$ A-mini-chaperone sample (data not shown). The  $\alpha$ A-mini-chaperone fibrils that formed were similar in appearance to that reported by Tanaka et al.<sup>23</sup> after the peptide chaperone had been shaken at 900 rpm for 24 h. Earlier we also observed fibril formation by  $\alpha$ A-crystallin peptides 66–80 and 67–75.<sup>30</sup> Because these peptides contain the core sequence <sup>71</sup>FVIFLD<sup>76</sup>, which also is homologous to the  $\beta$ -amyloid region integral to amyloid fibril formation,<sup>30</sup> one can surmise that the 71–76 region in  $\alpha$ A-crystallin drives fibril formation by these peptides. However, it is surprising that the CP1 peptide and the extended mini-chaperone, in spite of containing the FVIFLD sequence, did not form fibrils when they were incubated under similar conditions. Further, the results suggest that the addition of EEKPTSAPSS and VQEDFVEI affected the fibril formation by  $\alpha$ A-mini-chaperone.

Amyloid fibrils interact with ThT, and the resulting complex has increased fluorescence compared to that of ThT by itself.<sup>31</sup> When CP1 was treated with ThT, there was no increase in fluorescence, confirming the absence of an interaction between ThT and the peptide and the failure of CP1 to form fibril-like structures that are required for interaction with ThT (Figure 2B). As expected, the addition of ThT to  $\alpha$ A-mini-chaperone incubated for 72 h was associated with a 3-fold increase in fluorescence (Figure 2A). Such increased ThT fluorescence in the presence of  $\alpha$ A-mini-chaperone is consistent with TEM data that showed fibril formation by  $\alpha$ A-mini-chaperone and with the known correlation between ThT binding and fibril formation.<sup>23</sup> To examine whether the addition of the C-terminal sequence has any influence on the secondary structure of  $\alpha$ A-mini-chaperone, we performed secondary structural analysis of the peptide by CD spectrometry (Figure 4). Analysis of the far-UV CD spectrum of the chaperone peptide indicated that the  $\alpha$ A-mini-chaperone peptide has  $\beta$ -sheet structure, which was not displayed by CP1 or its truncated peptides. These results suggest that the C-terminal addition of two Glu residues to  $\beta$ -conformer peptide DFVIFLDVKHFS-PEDLT is sufficient to affect the secondary structure. The data further suggest that the  $\alpha$ A-crystallin C-terminal sequence EEKPTSAPSS or residues from this peptide, when they are fused to the C-terminus of mini-chaperone, a predominantly  $\beta$ -sheet peptide, impart a random structure to the peptide. Surprisingly, the extended mini-chaperone peptide, in spite of

having the full sequence of  $\beta$ -sheet-forming peptide, also did not show the CD conformation that reflects  $\beta$ -sheet formation. When one of the residues in the core region of a  $\beta$ -sheet-forming peptide is substituted with Pro (a  $\beta$ -sheet-breaking residue), the  $\beta$ -sheet conformation of the peptide is known to be completely abolished,<sup>32</sup> as was also demonstrated in our previous studies with  $\alpha$ A-mini-chaperone<sup>8</sup> as well as another  $\beta$ -sheet-forming peptide,  $\alpha$ A-66–80 derived from  $\alpha$ A-crystallin.<sup>30</sup> Substitution of Asp (corresponding to Asp-76) in  $\alpha$ A-mini-chaperone with isomers L- $\beta$ -, D- $\alpha$ -, and D- $\beta$ -Asp was found to change the  $\beta$ -sheet conformation into a random coil structure.<sup>22</sup> However, the fact that residues away from a peptide sequence with a propensity to form  $\beta$ -sheet structure influenced the conformation of the entire peptide in solution is surprising. In all likelihood, the interactions between amino acid residues from adjacent peptides are responsible for the apparent  $\beta$ -sheet conformation in  $\alpha$ A-mini-chaperone, whereas the lack of such interactions in CP1 or extended mini-chaperone peptide is responsible for random conformation in those peptides. Previously, it was reported that an 11-residue peptide can form either  $\alpha$ -helical or  $\beta$ -sheet structure when introduced into different locations in the primary sequence of the IgG-binding domain of protein G.<sup>33</sup> The IgG study suggested that the nonlocal interactions can determine the secondary structure of peptide sequences. Further studies are required to determine the role of specific amino acids in the CP1 peptide and their influence on the  $\beta$ -sheet conformation of  $\alpha$ A-mini-chaperone or truncated  $\alpha$ A-mini-chaperone peptide becoming a more random structure.

**Interaction of Bis-ANS with the CP1 Peptide.** The emission of bis-ANS, a hydrophobic site-specific probe, shifts to a lower wavelength, and the fluorescence increases when it interacts with proteins or peptides that possess significant hydrophobicity.<sup>34,35</sup> Binding of bis-ANS to the CP1 peptide resulted in an  $\sim$ 20% decrease in the emission maximum of the fluorophore (Figure 3). The bis-ANS binding property of CP1 was similar to that of the hydrophobic probe binding to  $\alpha$ A-mini-chaperone or  $\alpha$ B-mini-chaperones, as we reported previously.<sup>35</sup> However, the increase in bis-ANS fluorescence intensity observed with the CP1 peptide was  $\sim$ 20% lower than that recorded for  $\alpha$ A-mini-chaperone and bis-ANS (Figure 3). In contrast, the extended mini-chaperone showed significantly less bis-ANS fluorescence and a red shift in the emission maximum, indicating decreased hydrophobicity. Previous studies have shown that the chaperone activity of  $\alpha$ A-crystallin and mini-chaperone is affected when the mutations lead to weakened ANS or bis-ANS binding.<sup>3</sup> In our studies with the CP1 peptide, a slight decrease in the level of bis-ANS binding had no bearing on chaperone activity.

**Effect of the CP1 Peptide and Extended Mini-Chaperone on the Aggregation of Denaturing ADH, CS, and LA.** It is known that  $\alpha$ A-mini-chaperone and  $\alpha$ B-mini-chaperone, and their truncated forms, possess substrate-dependent chaperone activity.<sup>3,4,35</sup> Other studies have shown that both  $\alpha$ A- and  $\alpha$ B-crystallins also exhibit different degrees of chaperone efficiency with different client proteins.<sup>3,35</sup> We previously reported that truncation of  $\alpha$ A-mini-chaperone, by removing five residues from the N-terminal region or from the C-terminal region, leads to a significant reduction in chaperone activity.<sup>3,4</sup> This study clearly demonstrates that extension of the C-terminus of  $\alpha$ A-mini-chaperone ( $\Delta$ 87–88), via fusion of the  $\alpha$ A-crystallin C-terminal residues EEKPTSAPSS, does not diminish the chaperone-like activity of the mini-chaperone

toward client proteins ADH, CS, and LA, whereas a decrease in the length of the fusion peptide affects the chaperone activity. The loss of chaperone activity in the extended mini-chaperone peptide suggests that, in peptide chaperones, the residues adjacent to the chaperone sequence can also dictate the anti-aggregation activity of the peptide. Further, the findings suggest that a peptide with negligible  $\beta$ -sheet structure and significantly reduced bis-ANS binding capacity is not a chaperone. Tanaka et al.<sup>21,23</sup> have correlated the chaperone-like activity of  $\alpha$ A-mini-chaperone with its fibril formation property. This study shows that  $\alpha$ A-mini-chaperone can be modified in such a way that the new peptide will display chaperone activity when fibril forming capacity is compromised. The suppression of fibril formation capacity in CP1 may have an advantage over the original  $\alpha$ A-mini-chaperone in the development of mini-chaperones for clinical use because it is known that the peptide fibrils are undesirable *in vivo*.

**Mini-Chaperone Peptides Derived from  $\alpha$ -Crystallin Protect COS-7 Cells from Oxidative Injury.** The anti-apoptotic activity of mini-chaperones ( $\alpha$ A-mini-chaperone, CP1, and extended mini-chaperone) was evaluated in COS-7 cells. Cells were treated with peptide chaperones before being challenged with 150 mM H<sub>2</sub>O<sub>2</sub>, an oxidative agent, and apoptotic cells were analyzed by the TUNEL assay. The number of TUNEL-positive cells progressively decreased with increasing concentrations of chaperone peptides (Figure 8). At this time, the reason for the slight decrease in the anti-apoptotic activity of CP1 (after correcting for the higher molecular weight) is unclear.

**Protection of ARPE-19 Cells from H<sub>2</sub>O<sub>2</sub>-Mediated Oxidative Injury.** It is well-known that H<sub>2</sub>O<sub>2</sub> induces cell apoptosis via oxidative stress. To determine the effect of mini-chaperones on H<sub>2</sub>O<sub>2</sub>-induced cell apoptosis, we treated the ARPE-19 cells with 20  $\mu$ g/mL chaperone peptides before exposing the sample to 150  $\mu$ M H<sub>2</sub>O<sub>2</sub>. Apoptotic cells were probed using FITC-labeled annexin V and nuclear stain PI. The double-stained cells were analyzed by flow cytometry. The data show that mini-chaperones effectively protected the H<sub>2</sub>O<sub>2</sub>-induced apoptotic cascade in cells, consistent with TUNEL assay results. The data show  $>$ 50% protection against apoptosis with a peptide concentration of 20  $\mu$ g/mL at 24 h. Inhibition of apoptosis in COS-7 and ARPE-19 cells exposed to H<sub>2</sub>O<sub>2</sub> is likely through inhibition of caspase-3, because it has been shown that  $\alpha$ A-mini-chaperone blocks the conversion of procaspase into active caspase-3.<sup>10</sup>

## CONCLUSIONS

This is the first study to show that chimeric peptide CP1 is resistant to fibril formation, prevents protein aggregation, and protects cells from apoptosis. These results also suggest that  $\beta$ -sheet structure is not essential for the chaperone-like property of the  $\alpha$ A-crystallin-derived peptide chaperone.

## ASSOCIATED CONTENT

### Supporting Information

Elution profiles of chaperone peptides from a Sephadex G-50 column show the aggregation propensity of mini- $\alpha$ A but not CP1 peptide. This material is available free of charge via the Internet at <http://pubs.acs.org>.

## AUTHOR INFORMATION

### Corresponding Author

\*Department of Ophthalmology, EC213, University of Missouri School of Medicine, One Hospital Drive, Columbia, MO 65212. E-mail: sharmak@health.missouri.edu. Telephone: (573) 882-8478. Fax: (573) 884-4100.

### Funding

Supported by National Institutes of Health Grant EY023219.

### Notes

The authors declare no competing financial interest.

## ACKNOWLEDGMENTS

We thank Sharon Morey for help in the preparation of the manuscript.

## ABBREVIATIONS

LC-MS, liquid chromatography-mass spectrometry; RP-HPLC, reverse-phase high-power liquid chromatography; TEM, transmission electron microscopy; CPI, chimeric chaperone peptide DFVIFLDVKHFSPEDLTEEKPTSAPSS; H<sub>2</sub>O<sub>2</sub>, hydrogen peroxide; ADH, alcohol dehydrogenase; DTT, dithiothreitol; PC12, pheochromocytoma; RPE, retinal pigment epithelium; PI, propidium iodide; ThT, thioflavin T; sHSPs, small heat shock proteins; CS, citrate synthesis; LA,  $\alpha$ -lactalbumin; HEPES-KOH, 2-(hydroxyethyl)-1-piperazineethanesulfonic acid potassium hydroxide; EDTA, ethylenediaminetetraacetic acid; CD, circular dichroism; UV, ultraviolet; bis-ANS, 4,4'-bis(1-anilino-naphthalene 8-sulfonate); DMEM, Dulbecco's modified Eagle's medium; TUNEL, TdT-mediated digoxigenin-dUTP nick end labeling; PBS, phosphate-buffered saline; FITC, fluorescein isothiocyanate.

## REFERENCES

- (1) Lewis, R. J., and Garcia, M. L. (2003) Therapeutic potential of venom peptides. *Nat. Rev. Drug Discovery* 2, 790–802.
- (2) Antosova, Z., Mackova, M., Kral, V., and Macek, T. (2009) Therapeutic application of peptides and proteins: Parenteral forever? *Trends Biotechnol.* 27, 628–635.
- (3) Sharma, K. K., Kumar, R. S., Kumar, G. S., and Quinn, P. T. (2000) Synthesis and characterization of a peptide identified as a functional element in  $\alpha$ A-crystallin. *J. Biol. Chem.* 275, 3767–3771.
- (4) Kumar, R. S., and Sharma, K. K. (2000) Chaperone-like activity of a synthetic peptide toward oxidized  $\gamma$ -crystallin. *J. Pept. Res.* 56, 157–164.
- (5) Sreelakshmi, Y., and Sharma, K. K. (2001) Interaction of  $\alpha$ -lactalbumin with mini- $\alpha$ A-crystallin. *J. Protein Chem.* 20, 123–130.
- (6) Santhoshkumar, P., and Sharma, K. K. (2004) Inhibition of amyloid fibrillogenesis and toxicity by a peptide chaperone. *Mol. Cell. Biochem.* 267, 147–155.
- (7) Raju, M., Santhoshkumar, P., and Sharma, K. K. (2012)  $\alpha$ A-Crystallin-derived mini-chaperone modulates stability and function of cataract causing  $\alpha$ AG98R-crystallin. *PLoS One* 7, e44077.
- (8) Raju, M., Santhoshkumar, P., Henzl, T. M., and Sharma, K. K. (2011) Identification and characterization of a copper-binding site in  $\alpha$ A-crystallin. *Free Radical Biol. Med.* 50, 1429–1436.
- (9) Kannan, R., Sreekumar, P. G., and Hinton, D. R. (2012) Novel roles for  $\alpha$ -crystallins in retinal function and disease. *Prog. Retinal Eye Res.* 31, 576–604.
- (10) Sreekumar, P. G., Chothe, P., Sharma, K. K., Baid, R., Kompella, U., Spee, C., Kannan, N., Manh, C., Ryan, S. J., Ganapathy, V., Kannan, R., and Hinton, D. R. (2013) Antiapoptotic properties of  $\alpha$ -crystallin-derived peptide chaperones and characterization of their uptake transporters in human RPE cells. *Invest. Ophthalmol. Visual Sci.* 54, 2787–2798.

(11) Jeong, W. J., Rho, J. H., Yoon, Y. G., Yoo, S. H., Jeong, N. Y., Ryu, W. Y., Ahn, H. B., Park, W. C., Rho, S. H., Yoon, H. S., Choi, Y. H., and Yoo, Y. H. (2012) Cytoplasmic and nuclear anti-apoptotic roles of  $\alpha$ B-crystallin in retinal pigment epithelial cells. *PLoS One* 7, e45754.

(12) Xu, F., Yu, H., Liu, J., and Cheng, L. (2013)  $\alpha$ B-Crystallin regulates oxidative stress-induced apoptosis in cardiac H9c2 cells via the PI3K/AKT pathway. *Mol. Biol. Rep.* 40, 2517–2526.

(13) Hamann, S., Métrailler, S., Schorderet, D. F., and Cottet, S. (2013) Analysis of the cytoprotective role of  $\alpha$ -crystallins in cell survival and implication of the  $\alpha$ A-crystallin C-terminal extension domain in preventing Bax-induced apoptosis. *PLoS One* 8, e55372.

(14) Nahomi, R. B., Huang, R., Nandi, S. K., Wang, B., Padmanabha, S., Santhoshkumar, P., Filipek, S., Biswas, A., and Nagaraj, R. H. (2013) Acetylation of lysine 92 improves the chaperone and anti-apoptotic activities of human  $\alpha$ B-crystallin. *Biochemistry* 52, 8126–8138.

(15) Christopher, K. L., Pedler, M. G., Shieh, B., Ammar, D. A., Petrash, J. M., and Mueller, N. H. (2014)  $\alpha$ -Crystallin-mediated protection of lens cells against heat and oxidative stress-induced cell death. *Biochim. Biophys. Acta* 1843, 309–315.

(16) Nahomi, R. B., Wang, B., Raghavan, C. T., Voss, O., Doseff, A., Santhoshkumar, P., and Nagaraj, R. H. (2013) Chaperone peptides of  $\alpha$ -crystallin inhibit epithelial cell apoptosis, protein insolubilization and opacification in experimental cataracts. *J. Biol. Chem.* 288, 13022–13035.

(17) Slingsby, C., Wistow, G. J., and Clark, A. R. (2013) Evolution of crystallins for a role in the vertebrate eye lens. *Protein Sci.* 22, 367–380.

(18) Rehna, E. A., Singh, S. K., and Dharmalingam, K. (2008) Functional insights by comparison of modeled structures of 18 kDa small heat shock protein and its mutant in *Mycobacterium leprae*. *Bioinformatics* 3, 230–234.

(19) Laganowsky, A., Benesch, J. L., Landau, M., Ding, L., Sawaya, M. R., Cascio, D., Huang, Q., Robinson, C. V., Horwitz, J., and Eisenberg, D. (2010) Crystal structures of truncated  $\alpha$ A and  $\alpha$ B crystallins reveal structural mechanisms of polydispersity important for eye lens function. *Protein Sci.* 19, 1031–1043.

(20) Ecroyd, H., and Carver, J. A. (2009) Crystallin proteins and amyloid fibrils. *Cell. Mol. Life Sci.* 66, 62–81.

(21) Tanaka, N., Tanaka, R., Tokuhara, M., Kunugi, S., Lee, Y. F., and Hamada, D. (2008) Amyloid fibril formation and chaperone-like activity of peptides from  $\alpha$ A-crystallin. *Biochemistry* 47, 2961–2967.

(22) Fujii, N., Kida, M., and Kinouchi, T. (2010) Influence of L $\beta$ -, D $\alpha$ - and D $\beta$ -Asp isomers of the Asp-76 residue on the properties of  $\alpha$ A-crystallin 70–88 peptide. *Amino Acids* 39, 1393–1399.

(23) Fukuhara, S., Nishigaki, T., Miyata, K., Tsuchiya, N., Waku, T., and Tanaka, N. (2012) Mechanism of the chaperone-like and antichaperone activities of amyloid fibrils of peptides from  $\alpha$ A-crystallin. *Biochemistry* 51, 5394–5401.

(24) Pasta, S. Y., Raman, B., Ramakrishna, T., and Rao Ch, M. (2002) Role of the C-terminal extensions of  $\alpha$ -crystallins. Swapping the C-terminal extension of  $\alpha$ -crystallin to  $\alpha$ B-crystallin results in enhanced chaperone activity. *J. Biol. Chem.* 277, 45821–45828.

(25) Asthana, A., Raman, B., Ramakrishna, T., and Rao Ch, M. (2012) Structural aspects and chaperone activity of human HspB3: Role of the “C-terminal extension”. *Cell Biochem. Biophys.* 64, 61–72.

(26) Andley, U. P., Mathur, S., Griest, T. A., and Petrash, J. M. (1996) Cloning, expression, and chaperone-like activity of human  $\alpha$ A-crystallin. *J. Biol. Chem.* 271, 31973–31980.

(27) Takemoto, L., Emmons, T., and Horwitz, J. (1993) The C-terminal region of  $\alpha$ -crystallin: Involvement in protection against heat-induced denaturation. *Biochem. J.* 294, 435–438.

(28) Takemoto, L. (1994) Release of  $\alpha$ -A sequence 158–173 correlates with a decrease in the molecular chaperone properties of native  $\alpha$ -crystallin. *Exp. Eye Res.* 59, 239–242.

(29) Murugesan, R., Santhoshkumar, P., and Sharma, K. K. (2007) Cataract-causing  $\alpha$ AG98R mutant shows substrate-dependent chaperone activity. *Mol. Vision* 13, 2301–2309.



(30) Santhoshkumar, P., Raju, M., and Sharma, K. K. (2011)  $\alpha$ A-Crystallin peptide SDRDKFVIFLDVKHF accumulating in aging lens impairs the function of  $\alpha$ -crystallin and induces lens protein aggregation. *PLoS One* 6, e19291.

(31) Sulatskaya, A. I., Kuznetsova, I. M., and Turoverov, K. K. (2011) Interaction of thioflavin T with amyloid fibrils: Stoichiometry and affinity of dye binding, absorption spectra of bound dye. *J. Phys. Chem. B* 115, 11519–11524.

(32) Shamsir, M. S., and Dalby, A. R. (2007)  $\beta$ -Sheet containment by flanking prolines: Molecular dynamic simulations of the inhibition of  $\beta$ -sheet elongation by proline residues in human prion protein. *Biophys. J.* 92, 2080–2089.

(33) Minor, D. L., Jr., and Kim, P. S. (1996) Context-dependent secondary structure formation of a designed protein sequence. *Nature* 380, 730–734.

(34) Sudhakar, K., and Fay, P. J. (1996) Exposed hydrophobic sites in factor VIII and isolated subunits. *J. Biol. Chem.* 271, 23015–23021.

(35) Bhattacharyya, J., and Sharma, K. K. (2001) Conformational specificity of mini- $\alpha$ A-crystallin as a molecular chaperone. *J. Pept. Res.* 57, 428–434.